

Spatially Distributed Land-Use Efficiency Assessment under SDG Indicator 11.3.1: The Case of Greater Manila Area, Philippines

Jojene Santillan

Institute of Photogrammetry and GeoInformation
Leibniz University Hannover
Hannover, Germany

Caraga Center for Geo-Informatics & Department of Geodetic Engineering, College of Engineering and Geosciences,
Caraga State University, Butuan City, Philippines

jrsantillan@carsu.edu.ph

<https://orcid.org/0000-0002-5895-8647>

Meriam Makinano-Santillan

Caraga Center for Geo-Informatics & Department of Geodetic Engineering, College of Engineering and Geosciences,
Caraga State University, Butuan City, Philippines

mmsantillan@carsu.edu.ph

<https://orcid.org/0000-0002-5467-6722>

Preprint Notice

This manuscript is a non-peer-reviewed preprint submitted to EarthArXiv. It has also been submitted for review to the 12th International Exchange and Innovation Conference on Engineering & Sciences (IEICES 2026) and is currently under consideration. The content may be revised in response to the peer-review process.

Spatially Distributed Land-Use Efficiency Assessment under SDG Indicator 11.3.1: The Case of Greater Manila Area, Philippines

Jojene R. Santillan^{1,2}, Meriam Makinano-Santillan²

¹Institute of Photogrammetry and GeoInformation, Leibniz University Hannover, Germany, ²Caraga Center for Geoinformatics & Department of Geodetic Engineering, College of Engineering and Geosciences, Caraga State University, Butuan City, Philippines.
jrsantillan@carsu.edu.ph

Abstract: Sustainable Development Goal (SDG) Indicator 11.3.1 assesses urban land-use efficiency (LUE) through the relationship between land consumption rate (LCR) and population growth rate (PGR), commonly expressed as LCRPGR. However, city-level implementation produces a single value that can mask where efficient or inefficient urban development occurs. This study develops and demonstrates a spatially distributed approach to LUE assessment. Using the Greater Manila Area, Philippines, as a case study for 2000–2020, 100 m built-up area and population grids from the Global Human Settlement Layer were used to calculate local LCR, PGR, LCRPGR, and LUE regimes at the grid-cell level. Cells with valid initial built-up area and population values were assessed using the conventional LCR–PGR relationship, while cells transitioning from negligible to measurable values were classified as urban emergence zones. The resulting maps show that although aggregate LCRPGR indicates efficient land use at the metropolitan scale, cell-level analysis reveals localized inefficient expansion, population decline under stable or expanding built-up surfaces, and joint built-up and population emergence hidden in aggregate SDG 11.3.1 values.

Keywords: SDG 11.3.1; Land-use efficiency; Urban growth; Urban emergence.

1. INTRODUCTION

Urbanization continues to reshape landscapes worldwide, creating both opportunities and challenges for sustainable development [1]. As urban populations increase, cities expand spatially through the conversion of agricultural, forested, and other non-urban lands into built-up areas [2]. Understanding whether such expansion occurs efficiently relative to population growth has become an important concern for urban planners, policymakers, and international organizations [3]. To monitor this relationship, the United Nations established Sustainable Development Goal (SDG) Indicator 11.3.1, which measures land-use efficiency (LUE) through the interaction between land consumption and population growth [4].

Since its adoption, SDG 11.3.1 has become one of the most widely used indicators for evaluating urban development. The indicator is commonly implemented through the calculation of the land consumption rate (LCR), population growth rate (PGR), and the ratio between the two (LCRPGR) [4]. Numerous studies have employed Earth observation and population datasets to assess SDG 11.3.1 at local, national, regional, and global scales. In particular, the Global Human Settlement Layer (GHSL) has enabled consistent large-scale assessments by providing globally comparable built-up area and population datasets [5]. Recent work has demonstrated the usefulness of GHSL for evaluating urban growth and land-use efficiency across multiple reporting and analytical scales, including cities, urban centers, functional urban areas, countries, regions, and global urban systems [3, 6, 7].

Despite these advances, most SDG 11.3.1 applications continue to represent entire cities or urban centers using a single indicator value. While such aggregation facilitates reporting and comparison, it implicitly assumes that urban growth processes are spatially homogeneous [8]. In reality, cities are highly

heterogeneous environments. Dense urban cores, redevelopment districts, industrial zones, suburban neighborhoods, and peri-urban fringes frequently exhibit markedly different relationships between built-up expansion and population change, reflecting spatial variations in urban density, settlement age, and fringe development processes [9, 10]. Consequently, city-level indicators provide limited information regarding where efficient or inefficient urban development is occurring [8]. This limitation is particularly important because urban planning interventions are inherently spatial. Decisions concerning densification, infrastructure investment, transportation planning, and growth management require information on the location of urban growth processes rather than city-wide averages [11].

A second limitation becomes evident when SDG 11.3.1 is applied at finer spatial scales. Both LCR and PGR require non-zero initial values of built-up area and population. However, locations undergoing urban emergence frequently exhibit negligible or zero built-up area and population at the beginning of the analysis period. Under these conditions, the conventional growth-rate formulas become undefined. The interpretation of LCRPGR also becomes unstable in cells with stagnant or near-stagnant built-up area or population change [12]. In particular, when PGR approaches zero, even modest land consumption can produce extremely large LCRPGR values, making the indicator highly sensitive to small demographic changes [13]. Although these issues are generally less visible in city-level assessments, where total built-up area and population are rarely zero or near zero at the temporal endpoints of assessment, they become increasingly important in gridded analyses where newly urbanizing, stagnant, or near-stagnant cells are common. As a result, such cells require explicit methodological treatment rather than direct application of the conventional SDG 11.3.1 formula.

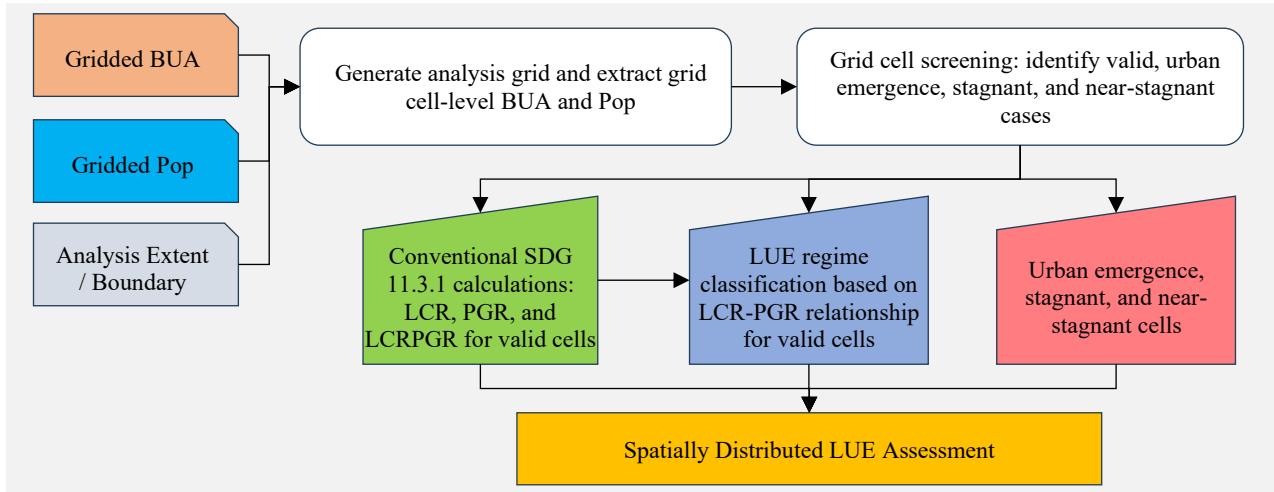


Fig. 1. Analytical framework for spatially distributed land-use efficiency assessment under Sustainable Development Goal (SDG) Indicator 11.3.1 using gridded built-up area (BUA) and population (Pop) data. Note: LCR–land consumption rate; PGR–population growth rate; LCRPGR–ratio of LCR to PGR.

The increasing availability of globally consistent Earth observation datasets [5] provides an opportunity to address these limitations through spatially distributed assessments of LUE. By calculating LCR, PGR, and related metrics at the level of regular grid cells rather than entire urban centers, it becomes possible to reveal localized patterns of densification, expansion, decline, and urban emergence. Such an approach complements conventional SDG 11.3.1 reporting by providing information on where specific urban growth processes are occurring.

This study proposes a gridded framework for spatially distributed LUE assessment. The framework integrates LCR, PGR, LCRPGR, built-up area per capita, and LUE regime classification within a common spatial framework, while explicitly accounting for cases where the conventional SDG 11.3.1 formulation becomes undefined or unstable. These include urban emergence zones with negligible initial built-up area or population, stagnant built-up area or population change, and near-zero PGR conditions that can produce inflated or unstable LCRPGR values.

The objectives of this study are therefore to: (i) develop a gridded framework for spatially distributed SDG 11.3.1 assessment; (ii) map local LUE regimes using cell-level LCR, PGR, and LCRPGR values; and (iii) identify and characterize urban emergence, stagnant, and near-stagnant cells that are not adequately represented by direct application of the conventional SDG 11.3.1 formulation.

By moving from aggregate indicators to spatially distributed assessments, this study aims to provide a more detailed understanding of urban growth dynamics and to demonstrate how gridded built-up area and population data can support more spatially explicit urban sustainability monitoring. The framework is subsequently demonstrated through an application to the Greater Manila Area (GMA) in the Philippines using GHSL built-up area and population datasets for 2000–2020.

2. THE SPATIALLY DISTRIBUTED LUE ASSESSMENT FRAMEWORK

2.1 Overview

The proposed framework extends conventional SDG 11.3.1 assessment from aggregate reporting units to spatially distributed analysis units. Rather than representing an entire city, urban center, or administrative unit with a single LCRPGR value, the framework evaluates the relationship between LCR and PGR at the level of individual grid cells. This enables the identification of localized urban growth patterns that aggregated assessments may conceal.

The framework integrates three main components: (i) identification of cells where the conventional SDG 11.3.1 formulation becomes undefined or unstable, including urban emergence and near-stagnant cells; (ii) calculation of the conventional SDG 11.3.1 metrics, including LCR, PGR, and LCRPGR; and (iii) classification of local LUE regimes based on the relationship between LCR and PGR.

Fig. 1 illustrates the overall workflow of the proposed framework. The framework requires built-up area (BUA) and population (Pop) data for at least two time periods. It can be implemented using any spatial dataset that provides these variables at a consistent spatial resolution.

2.2 Analysis Grid, Cell Screening, and Urban Emergence Mapping

The framework operates on a regular analysis grid. For each grid cell, BUA and Pop values are obtained for an initial time period, t_1 , and a final time period, t_2 . Before calculating the SDG 11.3.1 metrics, cells are screened to identify valid and special-case conditions. Cells with non-zero initial BUA and Pop are treated as valid LCR–PGR cells, including cases of BUA reduction and Pop decline, because these produce interpretable negative LCR and PGR values. Cells with zero initial BUA or Pop values but positive final values are treated separately as urban emergence zones. These zones are mapped to identify areas where built-up development or population presence emerged during the assessment period but where conventional LCR or PGR calculations are undefined. Cells with stagnant or near-stagnant BUA, Pop, or both are also flagged for special interpretation because they may later produce zero or near-zero LCR or PGR values, which can make the LCRPGR ratio unstable or difficult to interpret.

2.3 Conventional SDG 11.3.1 Metrics

For valid cells, the conventional SDG 11.3.1 metrics are calculated following the SDG 11.3.1 metadata [4]:

$$LCR = \frac{BUA_{t_2} - BUA_{t_1}}{BUA_{t_1}} \cdot \frac{1}{\Delta t} \quad (1)$$

$$PGR = \frac{\ln\left(\frac{Pop_{t_2}}{Pop_{t_1}}\right)}{\Delta t} \quad (2)$$

$$LCRPGR = \frac{LCR}{PGR} \quad (3)$$

In the above formulae, BUA and Pop denotes the cell built-up area and population at two epochs (t_1 and t_2), while Δt represents the time interval between [4].

2.4 LUE Classification

Valid cells are classified into LUE regimes based on the relationship between LCR, PGR, and LCRPGR. The classification scheme in Table 1 is based on and extends the regime framework of Santillan et al. [14]. Efficient LUE is defined as a condition in which land is not consumed unnecessarily relative to population change. Based on this definition, Regimes I–VII are classified as efficient because BUA either increases proportionally with Pop, increases more slowly than Pop, remains stable under Pop growth, or decreases relative to Pop change. Regimes VIII–XII are classified as inefficient because BUA is retained or expanded disproportionately relative to Pop change. Regime XIII is classified as neutral because both BUA and Pop remain stable. The resulting regime map can then be used to assess the spatial distribution of efficient, inefficient, and neutral LUE conditions.

2.5 Spatially Distributed LUE Assessment

The final component of the framework is the spatial assessment of LUE conditions across the analysis grid. This assessment combines the gridded SDG 11.3.1 metrics, LUE regime classes, and flagged special-case cells. Several analyses can be performed from these outputs. Maps of LCR, PGR, and LCRPGR can help identify where BUA expansion, Pop growth, and disproportionate land consumption are concentrated. The LUE regime map can be used to locate efficient, inefficient, and neutral areas and distinguishes the specific urban growth condition in each cell. Urban emergence maps can highlight locations where BUA or Pop shifted from zero or negligible initial values to measurable development.

The framework also allows summary statistics to be calculated, including the number and proportion of cells under each LUE regime, the spatial extent of efficient and inefficient conditions, and the prevalence of urban emergence and special-case cells. Together, these outputs provide information on where land is being consumed efficiently or inefficiently, where urban emergence is occurring, and how urban form interacts with local LUE conditions. Such information can support the identification of areas experiencing compact growth, potential overcrowding, inefficient expansion, urban decline, or emerging development, thereby providing a more comprehensive and spatially explicit assessment than aggregate city-level SDG 11.3.1 indicators alone.

classified according to the signs and relative magnitudes of LCR, PGR, and LCRPGR. General LUE classes are categorized as efficient (E), inefficient (I), neutral, or undefined (Und.). Efficient LUE refers to conditions in which land is not consumed unnecessarily relative to population change.

Regime	Name	LCR	PGR	LCRPGR	General LUE Class
I	Balanced Growth	+	+	= 1	E
II	Built-up Expansion under Faster Population Growth	+	+	0 < LCRPGR < 1	E
III	Population Growth Without Built-up Expansion	= 0	+	= 0	E
IV	Built-up Reduction under Population Growth	-	+	< 0	E
V	Built-up Reduction under Stable Population	-	= 0	Und.	E
VI	Faster Built-up Reduction under Slower Population Decline	-	-	> 1	E
VII	Proportional Built-up Reduction and Population Decline	-	-	= 1	E
VIII	Slower Built-up Reduction under Faster Population Decline	-	-	0 < LCRPGR < 1	I
IX	Stable Built-up Area under Population Decline	= 0	-	= 0	I
X	Built-up Expansion under Population Decline	+	-	< 0	I
XI	Built-up Expansion under Stable Population	+	= 0	Und.	I
XII	Built-up Expansion under Slower Population Growth	+	+	> 1	I
XIII	Neutral	= 0	= 0	Und.	Neutral

3. APPLICATION TO THE GREATER MANILA AREA, PHILIPPINES

3.1 Study Area

Table 1. Simplified LUE regime classification scheme based on and extended from Santillan et al. [14]. Regimes are

The Greater Manila Area (GMA) (Fig. 1) is a continuous urbanized region extending beyond the administrative boundaries of Metro Manila, the Philippines' National Capital Region. In this study, its boundary corresponds to the portion delineated as an urban center in the Global Human Settlement-Urban Center Database (GHS-UCDB) 2025, covering an area of 2,555 km². This boundary follows the Degree of Urbanization (DEGURBA) classification, which defines urban centers as contiguous built-up clusters with at least 50,000 inhabitants and a population density of at least 1,500 persons/km² [15]. The boundary includes adjacent portions of provinces of Bulacan and Pampanga to the north, Cavite and Laguna to the south, and Rizal to the east. GMA was selected because it contains Metro Manila, one of the largest, most densely populated, and most spatially heterogeneous urban regions in Southeast Asia [16]. The area is characterized by compact urban cores, industrial districts, and major transportation corridors, as well as less consolidated, rapidly developing peripheral areas. These characteristics make GMA an ideal environment for evaluating spatially distributed approaches to urban LUE assessment. Moreover, cities, provinces, and metropolitan areas within GMA, especially Metro Manila, have been the subject of numerous urbanization and sustainability studies, facilitating comparison with previous city-level analyses [7, 17, 18].

3.2 Datasets, Temporal Scope, and Analysis Grid

The framework was implemented using BUA and Pop datasets from the Global Human Settlement Layer (GHSL). BUA data were obtained from the GHS-BUILT-S product, while Pop data were obtained from the GHS-POP product, all from the GHSL Data Package 2023 [19]. In the GHSL framework, built-up surface refers to the gross surface bounded by the building wall perimeter, including the thickness of the walls, and corresponds to the commonly used term building footprint [19]. Accordingly, the GHS-BUILT-S product represents the amount of built-up surface within each grid cell, expressed in square meters, rather than a simple binary built-up/non-built-up classification.

The analysis utilized data for the years 2000 and 2020, corresponding to a 20-year assessment period. Both datasets are provided at a spatial resolution of 100 m, which was used as the analysis grid for characterizing spatial variations in urban growth, population dynamics, and LUE conditions within the GMA. At this resolution, each grid cell represents 10,000 m² of ground area, while the BUA value represents the estimated built-up surface amount contained within that cell.

This distinction is important for interpreting the results. In this study, BUA amount refers to the continuous built-up surface value within a grid cell and is used directly in calculating LCR. In contrast, built-up extent refers to the area represented by grid cells with measurable built-up and population presence based on the screening criteria applied to the continuous BUA and Pop values. Thus, existing built-up areas and urban emergence zones are categorical spatial classes derived from the continuous BUA and Pop surfaces. At the same time, the SDG 11.3.1 metrics are calculated using the underlying continuous values.

3.3 Framework Implementation

All spatial processing and metric calculations were

performed within the GMA analytical boundary using the 100 m analysis grid in Geographic Information System (GIS) environment (ArcGIS Pro 3.4). The procedures for cell screening, SDG 11.3.1 metric calculation, and LUE regime assignment followed the framework described in Section 2. The implementation generated cell-level maps and summary statistics for interpreting the spatial distribution of LUE conditions across GMA. These outputs form the basis of the results presented in the next section.

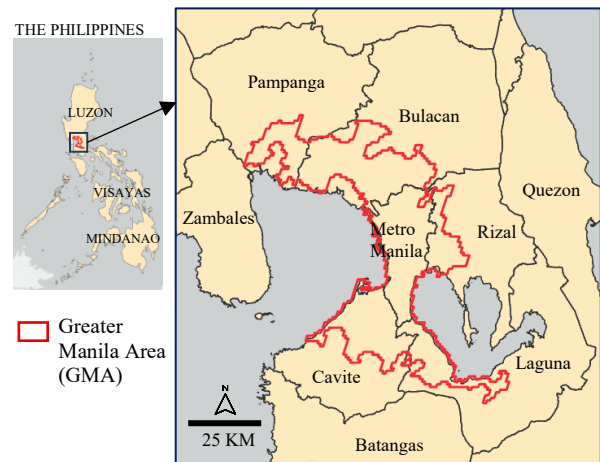


Fig. 1. Location and extent of the Greater Manila Area (GMA) urban center used as the study area, obtained from the GHS-Urban Center Database 2025 [15].

4. RESULTS

4.1 Existing Built-Up Areas and Urban Emergence Zones in the GMA, 2000–2020

At the aggregate level, the total BUA surface amount in the GMA, calculated from the continuous GHS-BUILT-S values, increased from about 374.22 km² in 2000 to about 422.41 km² in 2020. Over the same period, Pop increased from about 17.94 million to about 24.45 million. These aggregate changes indicate continued built-up surface and population growth across the metropolitan region. However, they do not show where established built-up and populated cells persisted, or where new ones emerged. The spatially distributed classification in Fig. 2 addresses this by separating existing built-up and populated cells, joint BUA–Pop emergence zones, and non-built-up areas.

The GMA was already predominantly built-up and populated during the assessment period, with existing built-up and populated cells covering 1,555.78 km², or 61% of the analytical boundary (Fig. 2). This value refers to the spatial extent of cells with established built-up and population presence, not the summed BUA surface amount. These cells form a large continuous built-up extent concentrated in Metro Manila and extending outward into the provinces of Pampanga, Bulacan, Rizal, Laguna, and Cavite. This pattern indicates that much of the region's built-up and populated footprint was already established by 2000 and remained part of the metropolitan system through 2020.

Joint BUA–Pop emergence zones covered 211.87 km², corresponding to 8% of the GMA. These zones are spatially concentrated along the margins of the existing built-up extent and appear as scattered patches in those locations. Their distribution suggests that new built-up and population growth during 2000–2020 occurred

mainly through outward expansion from Metro Manila and its surrounding built-up areas, with additional discontinuous growth in peripheral locations.

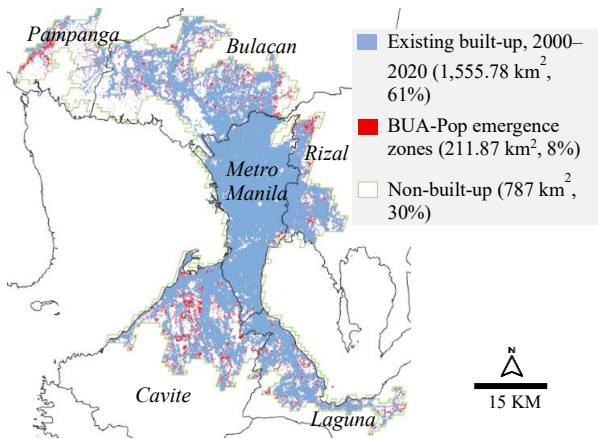


Fig. 2. Existing built-up areas, joint BUA–Pop emergence zones, and non-built-up areas in the GMA, 2000–2020.

Non-built-up areas accounted for 787 km², or 30% of the GMA analytical boundary. These areas are mostly located along the outer portions of the urban center boundary and represent areas that did not become jointly built-up and populated during the assessment period.

The existing built-up and populated cells also represent the valid cells used in the subsequent calculation of LCR, PGR, LCRPGR, and LUE regimes. In contrast, the joint BUA–Pop emergence zones are interpreted separately because they represent newly developed and newly populated cells rather than conventional LUE assessment cells with established initial BUA and Pop values.

4.2 Spatial Distribution of LCR

At the aggregate level, the GMA had an LCR of 0.64% per year during 2000–2020, indicating modest overall expansion of built-up surfaces across the metropolitan region. However, the spatial distribution of LCR shows that this aggregate value masks uneven built-up expansion within the valid cells (Fig. 3). Because LCR was calculated from the continuous BUA surface amount within each 100 m cell, the mapped values represent the rate of change in built-up surface, not the conversion of entire cells into built-up land. Cells with zero LCR accounted for 58% of the valid cells and are concentrated mainly in Metro Manila and other established built-up areas. These zero-LCR cells indicate no measurable change in BUA surface amount during the assessment period, although they may already contain built-up surfaces. This indicates that much of the central built-up extent had limited additional horizontal expansion during the assessment period, likely because many of these areas were already highly built-up by 2000.

Cells with low positive LCR values, corresponding to rates up to 1% per year, represented 17% of valid cells. These cells are distributed around the established built-up core and indicate areas of slow built-up expansion. Moderate LCR values, ranging from above 1% to 3% per year, accounted for 11% of valid cells and are more visible toward the northern, southern, and eastern portions of the GMA.

Higher LCR values were generally located along the margins of the existing built-up extent. Cells with LCR values above 3% to 5% per year comprised 4% of valid

cells, while those exceeding 5% per year accounted for 10%. These classes represent the most rapidly expanding built-up cells relative to their initial BUA surface amount. Because LCR is relative to the initial BUA value, high LCR values may occur in cells that had small initial built-up surface amounts but experienced a substantial proportional increase by 2020. Their spatial distribution indicates that rapid horizontal growth occurred mainly outside the central built-up core, particularly along peripheral expansion zones and metropolitan fringe areas.

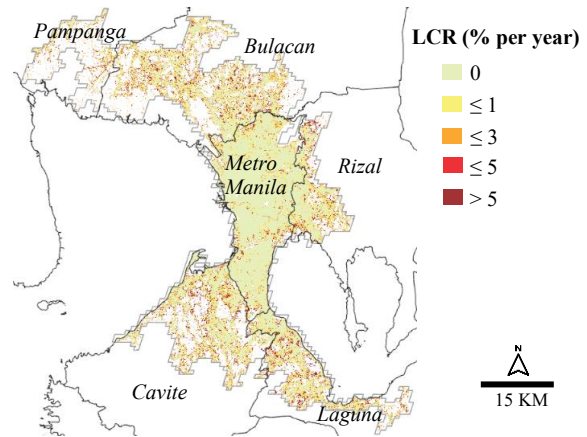


Fig. 3. Spatial distribution of LCR in the GMA, 2000–2020.

4.3 Spatial Distribution of PGR

Population growth in the GMA was generally positive during 2000–2020, with an aggregate PGR of 1.54% per year and a median cell-level PGR of 1.70% per year among valid cells. These values indicate overall population increase across the metropolitan region, but the gridded PGR pattern reveals important local differences in the intensity and direction of population change (Fig. 4).

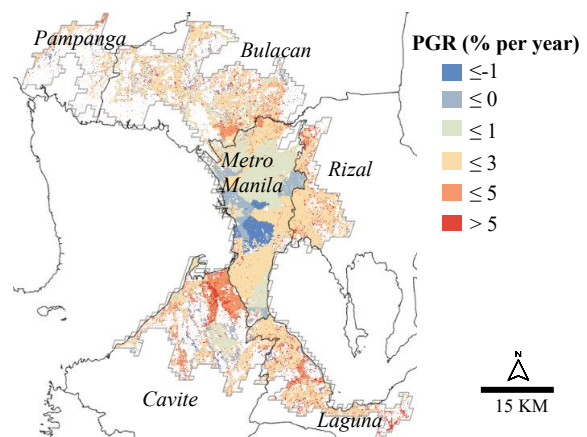


Fig. 4. Spatial distribution of PGR in the GMA, 2000–2020.

Most valid cells experienced positive population growth, with 44% of cells having PGR values above 1% to 3% per year and 22% having low positive PGR values up to 1% per year. These cells are widely distributed across Metro Manila and the surrounding provinces, indicating broad population increases across much of the existing built-up and populated extent.

Higher PGR values were more spatially clustered. Cells with PGR values above 3% to 5% per year accounted for 13% of valid cells, while cells exceeding 5% per year

represented 10%. These rapidly growing cells are more visible in parts of Cavite, Laguna, Bulacan, Rizal, and other peripheral areas, suggesting stronger population growth along these zones.

In contrast, cells with non-positive PGR accounted for 11% of valid cells, including 4% with PGR values below or equal to -1% per year and 7% with values above -1% to 0% per year. These cells are concentrated in selected cities within Metro Manila, particularly Makati, San Juan, Pasay, Marikina, and Malabon. The clustering of non-positive PGR values closely corresponds to city administrative boundaries, suggesting that part of this pattern may reflect the administrative population inputs used to generate the GHS-POP grids for the two reference years. Therefore, the observed population decline or near-stagnation in these areas should be interpreted as a gridded representation of city-level demographic change, rather than as purely cell-level population redistribution.

Overall, the PGR map reveals widespread population growth across the GMA, especially in outer areas, but also highlights localized population decline or weak growth within selected established urban areas of Metro Manila. This spatial pattern provides important context for interpreting LCRPGR and LUE regimes, because low or negative PGR can strongly affect the ratio-based assessment of land-use efficiency.

4.4 Spatial Distribution of LCRPGR and LUE Regimes

The aggregate LCRPGR value for the GMA was 0.42 during 2000–2020. Since both aggregate LCR and PGR were positive, as shown in Sections 4.2 and 4.3, this value indicates efficient land use at the aggregate level, with population growth exceeding land consumption. However, this single value does not show how the relationship between built-up surface expansion and population growth varied across the GMA.

The spatial distribution of LCRPGR shows that low and non-positive values dominated the valid cells during the same period (Fig. 5). Cells with LCRPGR values less than or equal to zero accounted for more than half of the valid cells, mainly because 58% of valid cells had zero LCR. These values, therefore, largely reflect cells with no measurable increase in BUA surface amount, although the corresponding Pop dynamics varied across locations. Cells with LCRPGR values between 0 and 1 indicate areas where Pop growth was faster than built-up surface expansion, while values above 1 indicate areas where built-up surface expansion outpaced Pop growth. The latter are more visible in the outer, less consolidated portions of the GMA urban center, where horizontal expansion was more active during the assessment period. However, the LCRPGR map alone does not fully explain local LUE conditions because it hides the sign combinations of LCR and PGR. For example, negative LCRPGR values may result from very different situations, such as built-up expansion with population decline or built-up reduction with population growth. Thus, the LUE regime map in Fig. 6 provides a more informative interpretation by combining the signs and relative magnitudes of LCR, PGR, and LCRPGR according to the classification scheme shown in Table 1. The regime map (Fig. 6) shows that the valid cells were dominated by efficient LUE conditions. The largest share was *Regime III: Population Growth Without Built-up*

Expansion, accounting for 49% of valid cells. This regime is concentrated mainly in Metro Manila and other established built-up areas, indicating locations where Pop increased while the BUA surface amount remained stable. This pattern suggests efficient land use in ratio terms, although it may also reflect limited remaining space for additional horizontal expansion in already highly built-up areas.

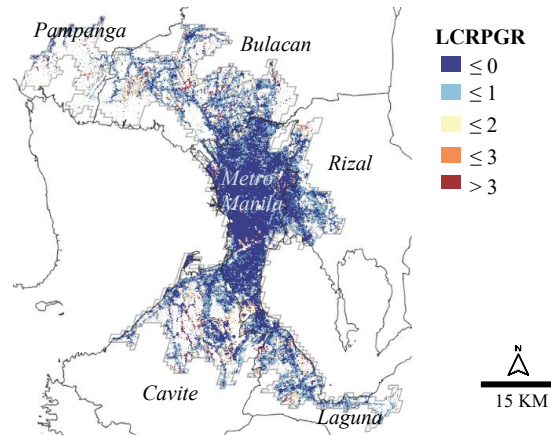
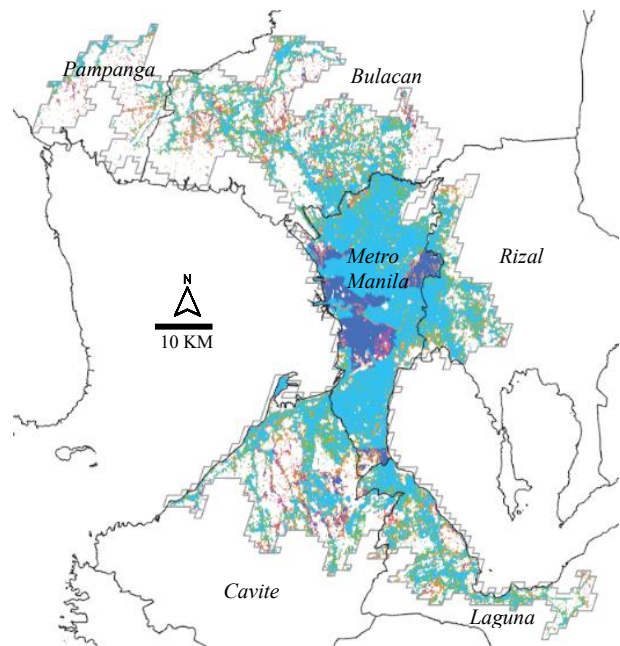


Fig. 5. Spatial distribution of LCRPGR in the GMA, 2000–2020.



LUE Regimes:

- II. Built-up Expansion under Faster Population Growth (26%)
- III. Population Growth Without Built-up Expansion (49%)
- IX. Stable Built-up Area under Population Decline (9%)
- X. Built-up Expansion under Population Decline (2%)
- XII. Built-up Expansion under Slower Population Growth (14%)

Fig. 6. Spatial distribution of LUE regimes in the GMA, 2000–2020. Regimes were assigned to valid cells based on the cell-level relationship between LCR, PGR, and LCRPGR. The percentage values in the legend indicate the share of each regime among valid cells.

The next largest share was *Regime II: Built-up Expansion under Faster Population Growth*, representing 26% of valid cells. These cells indicate areas where both BUA and Pop increased, but Pop grew faster than BUA. Spatially, this regime appears around the established

built-up extent and in the outer portions of the GMA urban centre, suggesting continued growth with relatively efficient land consumption.

In contrast, inefficient conditions were mainly represented by *Regime XII: Built-up Expansion under Slower Population Growth*, which accounted for 14% of valid cells. These areas indicate locations where BUA surface expansion outpaced Pop growth and are more visible along the margins of the existing built-up extent. Smaller shares were classified as *Regime IX: Stable Built-up Area under Population Decline* at 9% and *Regime X: Built-up Expansion under Population Decline* at 2%. These regimes indicate localized areas where Pop declined despite stable or expanding BUA surface amounts.

Overall, the regime map shows that most valid cells experienced either population growth without additional built-up expansion or built-up expansion that was slower than population growth. However, it also identifies localized inefficient conditions that are not clearly distinguishable from the LCRPGR map alone, particularly where built-up expansion occurred under slower or declining population growth.

5. DISCUSSION

The results demonstrate the importance of interpreting SDG 11.3.1 beyond a single aggregate LCRPGR value. Although the aggregate indicator suggests efficient land use in the GMA during 2000–2020, the cell-level assessment showed that this overall pattern was composed of different local conditions, including established built-up areas, localized expansion, population decline, and joint BUA–Pop emergence. Thus, aggregate LUE assessment can summarize the overall relationship between land consumption and population growth, but it may conceal where specific urban growth processes occur within the urban center.

The spatial patterns observed in the GMA reflect a highly urbanized region with a consolidated built-up core and continuing outward development in less consolidated portions of the urban center. This reinforces the need for spatially distributed assessment, since metropolitan-scale averages cannot adequately represent the coexistence of stable built-up areas, emerging built-up and populated cells, and localized inefficient expansion. The clustering of non-positive PGR in selected Metro Manila cities also suggests that gridded population patterns may partly reflect the administrative population inputs used in generating GHS-POP, rather than purely cell-level redistribution.

The LCRPGR map provides a useful summary of the relationship between land consumption and population growth, but it is insufficient on its own for interpreting local LUE conditions. Similar LCRPGR values can result from different LCR and PGR sign combinations; for example, negative LCRPGR may indicate either built-up expansion with population decline or built-up reduction with population growth. The LUE regime map addresses this limitation by combining the signs and relative magnitudes of LCR, PGR, and LCRPGR. This is consistent with sign-based interpretation approaches used in previous studies, where positive, zero, and negative combinations of LCR, PGR, and LCRPGR are distinguished to separate population-driven densification, land-intensive expansion, and expansion under population decline [7, 20].

The proposed framework, therefore, complements existing responses to the limitations of SDG 11.3.1. Some studies address LCRPGR instability by examining empirical value distributions, filtering or bounding extreme values, or aggregating results to larger spatial units to reduce the influence of extreme local outcomes [7, 21, 22]. Other work has questioned whether LCRPGR should remain the primary summary metric. Zhong et al. [13], for example, emphasized the use of built-up area per capita (BPC) and related derivatives because they tend to yield smoother and more stable temporal patterns than LCRPGR. Angel et al. [12] proposed replacing the ratio-based indicator with rate-based measures of land consumption per person and population density change. In contrast, the present framework retains the conventional SDG 11.3.1 components; it improves their spatial interpretation by mapping specific LCR–PGR relationships and separating cells where direct ratio-based interpretation is problematic.

These findings also have practical implications for spatial planning and SDG monitoring. Cells where Pop increased without additional built-up surface expansion may indicate compact growth, overcrowding, redevelopment, or limited remaining space for horizontal expansion, while areas where built-up surface expanded faster than Pop may require closer attention for land-use regulation, infrastructure efficiency, and growth management. Cells with stable or expanding built-up surface under population decline may indicate potential underutilization or demographic restructuring. Joint BUA–Pop emergence zones are also important because they identify newly developed and newly populated locations that may require infrastructure provision, service planning, and continued monitoring of future land consumption.

6. CONCLUSIONS AND OUTLOOK

This study demonstrated a spatially distributed framework for assessing LUE using gridded BUA and Pop data. Applied to the GMA, the framework showed that aggregate SDG 11.3.1 values can conceal substantial local variation in built-up surface expansion, population growth, urban emergence, and LUE regimes. By distinguishing valid LCR–PGR cells, joint BUA–Pop emergence zones, and specific LUE regimes, the framework provides a more spatially explicit basis for interpreting where efficient and inefficient land-use conditions occur within an urban center.

Several limitations should be noted. First, the results depend on the quality and spatial detail of the gridded BUA and Pop datasets. The GHS-BUILT-S product represents a continuous built-up surface amount within each cell. In contrast, the mapped built-up extent in this study represents the area of cells with measurable built-up and population presence. These two quantities should not be interpreted as equivalent. Second, gridded population patterns may reflect the administrative units and redistribution methods used to produce GHS-POP, as suggested by the clustering of non-positive PGR values along selected city boundaries. This indicates that spatially distributed LUE assessment requires carefully generated gridded population data, preferably using fine-scale dasymetric redistribution or building-level ancillary information rather than coarse administrative allocation alone. Third, the results are scale-dependent because the framework was implemented at 100 m resolution.

Different grid sizes, thresholds, or input datasets may produce different local classifications. Future work can therefore test the framework using alternative gridded datasets, finer-resolution population redistribution methods, and additional urban centres to assess its robustness and transferability.

7. REFERENCES

- [1] B. Venkatesh, R. Velkennedy, S. Murugan, and A. Velmurugan, "Indicator for formulating and measuring the Urban Sustainability Index: A Review," *Proceedings of International Exchange and Innovation Conference on Engineering & Sciences (IEICES)*, vol. 9, pp. 447–452, Oct. 2023, doi: 10.5109/7158038.
- [2] M. Salem and N. Tsurusaki, "Empowering sustainability: Innovative deep learning and remote sensing solutions for urban monitoring and sustainable development," *Proceedings of International Exchange and Innovation Conference on Engineering & Sciences (IEICES)*, vol. 9, pp. 391–396, Oct. 2023, doi: 10.5109/7158006.
- [3] R. C. Estoque, M. Ooba, T. Togawa, Y. Hijioka, and Y. Murayama, "Monitoring global land-use efficiency in the context of the UN 2030 agenda for sustainable development," *Habitat International*, vol. 115, 2021, doi: 10.1016/j.habitatint.2021.102403.
- [4] UN Statistics Division, "SDG indicator metadata (Harmonized metadata template – format version 1.0). Last updated 2025-04-23." Accessed: Oct. 05, 2025. [Online]. Available: <https://unstats.un.org/sdgs/metadata/files/Metadat a-11-03-01.pdf>
- [5] M. Pesaresi *et al.*, "Advances on the global human settlement layer by joint assessment of earth observation and population survey data," *International Journal of Digital Earth*, vol. 17, no. 1, 2024, doi: 10.1080/17538947.2024.2390454.
- [6] M. Schiavina *et al.*, "Land use efficiency of functional urban areas: Global pattern and evolution of development trajectories," *Habitat International*, vol. 123, 2022, doi: 10.1016/j.habitatint.2022.102543.
- [7] J. R. Santillan and C. Heipke, "Assessing patterns and trends in urbanization and land use efficiency across the Philippines: a comprehensive analysis using global earth observation data and SDG 11.3.1 indicators," *PFG - Journal of Photogrammetry, Remote Sensing and Geoinformation Science*, 2024, doi: 10.1007/s41064-024-00305-y.
- [8] M. Schiavina *et al.*, "Multi-scale estimation of land use efficiency (SDG 11.3.1) across 25 Years Using Global Open and Free Data," *Sustainability (Switzerland)*, vol. 11, no. 20, 2019, doi: 10.3390/su11205674.
- [9] J. Péntzes, L. D. Hegedűs, K. Makhanov, and Z. Túri, "Changes in the patterns of population distribution and built-up areas of the rural–urban fringe in post-Socialist context—A Central European case study," *Land*, vol. 12, no. 9, p. 1682, Aug. 2023, doi: 10.3390/land12091682.
- [10] H. Taubenböck, J. Mast, R. Lemoine Rodríguez, H. Debray, M. Wurm, and C. Geiß, "Was global urbanization from 1985 to 2015 efficient in terms of land consumption?," *Habitat International*, vol. 160, p. 103397, Jun. 2025, doi: 10.1016/j.habitatint.2025.103397.
- [11] OECD, *Rethinking Urban Sprawl: Moving Towards Sustainable Cities*. OECD, 2018. doi: 10.1787/9789264189881-en.
- [12] S. Angel, E. Mackres, and B. Guzder-Williams, "Measuring change in urban land consumption: a global analysis," *Land*, vol. 13, no. 9, p. 1491, Sep. 2024, doi: 10.3390/land13091491.
- [13] C. Zhong, L. Peng, J. Yu, I. Swan, and Li, "Toward more reliable, complete, and equitable global urban land use efficiency assessments," *Commun Earth Environ*, vol. 6, no. 1055, 2025.
- [14] J. Santillan, M. Dorozynski, and C. Heipke, "Enhancing land use efficiency assessment through built-up area–built-up volume trajectories: integrating vertical urban growth into SDG 11.3.1 monitoring," *IJGI*, vol. 14, no. 10, p. 404, Oct. 2025, doi: 10.3390/ijgi14100404.
- [15] European Commission *et al.*, "Stats in the City the GHSL Urban Centre Database 2025," Publications Office of the European Union, Luxembourg, 2024. doi: <https://data.europa.eu/doi/10.2760/3046391>.
- [16] A. Murakami, A. Medrial Zain, K. Takeuchi, A. Tsunekawa, and S. Yokota, "Trends in urbanization and patterns of land use in the Asian mega cities Jakarta, Bangkok, and Metro Manila," *Landscape and Urban Planning*, vol. 70, no. 3-4 SPEC., pp. 251–259, 2005, doi: 10.1016/j.landurbplan.2003.10.021.
- [17] A. Olfato-Parojinog, P. A. Sobremonte-Maglipon, J. E. Limbo-Dizon, K. J. Almadrones-Reyes, and N. H. A. Dagamac, "Land use/land cover changes (LULCC) using remote sensing analyses in Rizal, Philippines," *GeoJournal*, vol. 88, no. 6, pp. 6105–6118, 2023, doi: 10.1007/s10708-023-10959-7.
- [18] A. Olfato-Parojinog, N. H. A. Dagamac, and J. E. Limbo-Dizon, "Assessment of urban green spaces per capita in a megacity of the Philippines: implications for sustainable cities and urban health management," *GeoJournal*, vol. 89, no. 3, p. 94, Apr. 2024, doi: 10.1007/s10708-024-11084-9.
- [19] European Commission, "GHSL Data Package 2023," Publications Office of the European Union, Luxembourg, 2023. doi: 10.2760/098587.
- [20] H. Jiang *et al.*, "An assessment of urbanization sustainability in China between 1990 and 2015 using land use efficiency indicators," *npj Urban Sustainability*, vol. 1, no. 1, p. 34, Dec. 2021, doi: 10.1038/s42949-021-00032-y.
- [21] B. Calka, A. Orych, E. Bielecka, and S. Mozuriunaite, "The Ratio of the Land Consumption Rate to the Population Growth Rate: A Framework for the Achievement of the Spatiotemporal Pattern in Poland and Lithuania," *Remote Sensing*, vol. 14, no. 5, 2022, doi: 10.3390/rs14051074.
- [22] C. Li, G. Cai, and M. Du, "Big data supported the identification of urban land efficiency in eurasia by indicator SDG 11.3.1," *ISPRS International Journal of Geo-Information*, vol. 10, no. 2, 2021, doi: 10.3390/ijgi10020064.